Model Updating Based on Static and Ground Vibration Tests of a Blended Wing Body Aircraft

Gonçalo Rodrigues de Araújo
goncalo.de.araujo@tecnico.ulisboa.pt

Instituto Superior Técnico, Universidade de Lisboa, Portugal

January 2021

Abstract

Over the past few decades, the aviation industry has been exploring new aircraft configurations for optimal environmental performance. During the conceptual design phase, estimation on the performance and flightworthiness of these novel configurations can be attained by using scaled flight demonstrators. The Blended Wing Body (BWB) concept consists of a hybrid architecture aircraft and it presents considerable advantages in aerodynamic efficiency. The University of Victoria Center for Aerospace Research (UVic-Cfar) is developing an Unmanned Aerial Vehicle (UAV) that represents a 16.5 % scaled flight test model to quantify flight performance and optimize flight control strategies.

This thesis presents experimental static and Ground Vibration Tests (GVT) studies on the BWB wing and an update of the finite element model for the wing structure. The goal is to correlate the simplified FEM with the static and dynamic behavior of the real structure as manufactured. This updated model will be subsequently used for aeroelastic studies. Different models that accurately represent the behaviour of the wing structure were obtained, however, some challenges were identified when trying to match the computational and experimental dynamic mode shapes.

Keywords: Blended Wing Body, Static Load Tests, Ground Vibrations Tests, Experimental Modal Analysis, Finite Element Models Update.

1. Introduction

Nowadays, aeronautics and aerospace are one of the most advanced engineering fields where there is a need to unceasingly improve and find solutions for new optimized designs with a strong hope to get solutions to implement in a near future.

Bombardier Aeroespace is pushing researchers and developers to explore a new configuration called BWB. This hybrid architecture take advantadge of the benefits of a flying wing accompanied with the benefits of a traditional aircraft: "has a more obvious centerbody, highly aerodynamic efficient outer wing providing part of the lift, and a smoothly blended (integrated) region in between."[1].

Other companies, specially in United States of America (USA), Boeing, National Aeronautics and Space Administration (NASA), universities (Stanford, South California, Florida and Clark-Atlanta) and also Airbus, outside of the USA, are some of the entities that are researching and the results indicate: "a significant difference in potential aerodynamic performance.". Passenger planes have not been manufactured yet with this configuration but one of the aircraft called X-48B and was developed by a partnership between NASA and Boeing, previously flown a scaled model. DZYNE Ascent 1000 and DZYNE BWB-XLC are other BWB aircraft examples that have been proposed in the last decade[2].

After the success obtained by UVic-Cfar with the manufacturing and testing of the 7% scaled BWB aircraft, the project evoluted to a higher level of complexity with the buildup of the 16.5% scaled aircraft. This new prototype, is a 5.4 meters wingspan aircraft, currently under development. The content of this thesis is part of this prototypes wing ground testing, one of the fundamental assignments for the validation of the previously designed model.

Being this innovative project such a complex aircraft with 24 control surface devices and approximately 5.4 m wingspan, the motivation for this document is to generate and optimize the properties of a beam Finite Element Model (FEM) in order to match as well as possible the static and dynamic response of the original wing structure.

Trying to achieve the high level of similarity between both models, mass, inertia and stiffness of structures as well as natural frequencies and modes can be quantified resorting to static load tests and Ground Vibration Tests (GVT) that are

also important to update the characteristics of the beam model developed. Model updating and tuning based on experimental results increases the confidence on the model and subsequent results obtained from its use [3].

To the best of the author's knowledge, the study of the differences between beam models generated from static load behaviour and modal response, in such complex wing structure, was never performed previously, neither using computational tools or experimental response correlation.

This document's work reports a comparison of static load tests and GVT results with the corresponding predicted results based on the wing's Finite Element Analysis (FEA), followed by the process to generate and update a simplified beam model for a future aeroelastic dynamic instability boundary calculation.

2. Background

UAVs are aircraft operated without human pilot on board and have been one of the technologies that is exponentially growing in the past decade. The military sector was the pioneer and responsible for the earlier developments and nowadays there are developed applications on sensing, mapping, goods and equipment delivery, inspection and monitoring. The advantages of not having a human on board of the aircraft can accelerate and manoeuvrer beyond the limits permitted by human biology [4]. This typology of aircraft is pronouncing a wide use in aerospace companies as flight test proof for concept validation, as is the case in this study.

2.1. Static Load Testing

Static aeroelasticity models the coupling effect between elastic and aerodynamic forces. It considers the non oscillatory effect of forces applied on a structure. The stiffness of the wing will influence the in-flight wing shape and consequent lift distribution, either in cruise flight or performing specific manoeuvres. However, sometimes aerodynamic calculations and computational simulations (even accurate ones) can induce errors if the structure model is not perfectly representing the test article. To tackle these differences, static tests are the best operation to confirm and validate the data [5].

This process goes over a test plan where a simplified representative of the desired load case is studied followed by the choice of the location to measure the responses. This selection is done with the help of a preliminary static analysis of the FEM. Designing a static rig is fundamental to ensure a compatibility of substructures' displacements and a force equilibrium on substructures' interface degrees of freedom (DOFs). It is important to have the same boundary conditions in the experimental tests and in the FEM analysis.

The innovative part of static ground testing is on the method used to get the experimental data with high levels of accuracy when measuring the displacements. Visual Image Correlation (VIC) measures the displacements and local deformation comparing analogue representations of photographs [6]. Photogrammetry method consists in getting precise measurements from photographs of an object and it has been recently used to perform 3D digitizing of tests objects for testing applications [7]. The process is similar to VIC and consists in two or more cameras to get spacial motion. Experiments with this method on wings was already performed earlier [8].

This method used in this work to get the displacements during the wing static loading ground tests was a metrology 3-dimensional scanning method in different load cases using a grade optical Coordinate Measuring Machine (CMM). It results in high accuracy results, in the same order as photogrammetry but with a simpler tool. Recent studies using this method on aircraft testing were already done [9].

2.2. Modal Analysis

Modal analysis makes the study easier when converting an utterly bewildering vibration signal of excitation and responses measurements into a simple set of parameters clear to visualize. It is in practice the identification of natural frequencies, damping ratios and mode shapes of a structure coming out of FRF measurements [10].

Non linear modal analysis of a full scaled aircraft was already done [11][10] and states that stiffness non linearities induced by structural deformations are not significant at small deformations, as in this case of study.

Modal analysis begins with the calculation of an undamped case, where the Newton's equation 1 is simplified neglecting the damping matrix and considering a free vibrating system. When analysing a general damped case, the complete Newton's equation 1 will be considered.

$$[M]\{u^{''}(t)\} + [C]\{u^{'}(t)\} + [K]\{u(t)\} = \{f(t)\} \quad (1)$$

Where $[M]$, $[C]$ and $[K]$ are the mass, damping and stiffness matrices, respectively. $\{f\}$ is the vector of externally applied forces and $\{u^{''}(t)\}$ and $\{u^{'}(t)\}$ corresponds to the second and first derivative of $\{u(t)\}$, being $\{u(t)\}$ the vector of displacements.

If equation 1 is equalled to zero, the free vibrations of the system may be solved. Applying the Laplace Transform it is possible to solve the eigensystem and to represent each mode, the second pole from the conjugate pair is considered with the positive imaginary part being written as:

$$s_R = -\zeta_R \omega_R + j\omega_R \sqrt{1-\zeta_R^2} \quad (2)$$

Where ζ_R is the damping coefficient and the angular frequency ω_R is often presented in terms of cycles as $f_R = \frac{\omega_R}{2\pi}$. Each natural frequency is associated to a specific mode and represents a frequency at which the structure resonates [12].

Lanczos Method is a efficient algorithm to perform a modal analysis for large models, it is a fast and robust algorithm and used for most applications as the default solver [13].

2.3. Ground Vibration Testing

Dynamic Aeroelasticity results from the coupling between elastic and inertia forces and considers the oscillatory effect of forces applied on a structure, fundamental for predicting the occurrence of the tragic phenomenon called flutter[5].

Experimental Modal Analysis (EMA), GVT in this case, assures that no adverse dynamics behaviour occurs. It consists in the experimental measurement of an aircraft structural vibration modes including peak frequencies, damping and mode shapes and the goal is to identify flutter, detect structural flaws and identify flight control dynamic problems.

Because of the relevance of this topic, international research was done [10] and recent methods have been studied for different types of aircrafts [9].

The Transfer Function (TF) is a mathematical model representing the relationship between two signals, the excitation and the response of a physical system. Can be defined as $H(s) = \dfrac{Y(s)}{X(s)}$, where $Y(s)$ and $X(s)$ are the Laplace transforms of the output and input, respectively.

The FRF, used on the EMA, is mathematically the Fourier transform of the output divided by the Fourier transform of the input. FRFs are obtained by evaluating the imaginary axis of the Laplace domain where $s = j\omega$. The frequencies at which the structure vibrates freely are obtained from the poles of the TF.

FRF has advantages compared to TF because it can be experimentally measured. The acceleration response of the structure is measured relative to the force excitation from the impact hammer in the time domain but it can be transformed into frequency domain using the Fast Fourier Transform (FFT) [14].

An important phenomenom called leackage may occurs when a signal is aperiodic and can results in frequency and magnitude errors. Averaging, increasing frequency resolution, use periodic excitation and the use of time domain windowing functions can be solutions to this problem.

FRFs are expressed in a Bode Diagram with magnitude measured in g/N and phase diagram expressed in degrees.

$$Amplitude = \sqrt{Imag^2 + Real^2} \quad (3)$$

$$Phase = tan^{-1}\left(\frac{Imag}{Real}\right) \quad (4)$$

To plot the mode shape, more than one FRF is acquired at different locations on the structure and they are all phased with respect to the imaginary part.

More than one impact at the some point is important to have a coherence graphic, used to assess the quality of measurements displaying the average similarity level between the impacts and the FRFs. It tells what portion of the response is attributed to the excitation and should ideally be higher than 0.9 [15].

Two main types of excitation can be done, impact testing or shaker testing. In theory, there is no differnece between the type of resutls.

Impact testing consists in directly hit the structure with an impact hammer with an embedded impedance head that measures the force[11]. While an impact is being done, high sensitivity accelerometers distributed along the wing measure the response to the excitation.

Impact testing was chosen for this experimental work because the acquisition and control is way simpler and small complexity of the setup. In fact, the only advantage of a shaker testing is that it gives the user an accurate control over the inputs. A problem called mass loading, a phenomenon where the mass of the devices used to measured the responses affects the vibrations of the structure, can appear while shaker testing [12]. This structure is a stiff wing with very low flexibility and good results can be achieved with impact tests.

Roving hammer means that a single or multiple response/s DOF is/are fixed and the excitation is roving around test points. Roving accelerometer means that the excitation source will be always in the same point and everytime there is an impact, the measuring sensor moves to other test point. A single DOF is enough to get the correct dynamics results and Maxwell's reciprocity states that both methods achieve the same results [16]. In order to avoid the need of always move the transducers once they are glued, roving hammer method was used.

Data acquisition was accomplished using National Instruments NI cDAQ-9188 with IEPE NI 9234 acquisition cards to connect the accelerometers and the impact hammer. Conversion and amplification of analogue signals into digital systems is responsibility of *LabVIEW* software that stores in

the system's memory one data block for each measured DOF impacted.

During the pre testing and development of the test strategy, it is important to perform a computational modal analysis of the jig to make sure the natural frequencies are in a different range of the ones expected for the structure. A functionality of *FEMtools* called Sensor Elimination Algorithm by Modal Assurance Criteria (SEAMAC) was the method used to choose the accelerometers placement, in order to avoid nodal points.

Modal parameters extraction can be done in a sequence of identifying the normal modes followed by least-squared curve-fit to get the natural frequencies and modal damping values and finishing with a refined curve-fit to determine the mode shapes [11].

Curve fitting is a data reduction process that converts the dynamic information from a set of FRFs into a set of modal parameters, with the help of *MEScope* software.

A ressonance is identified as a peak in the magnitude of the FRF. The wider the peak, the heavier the damping, with the damping ratio calculated as $\zeta_R = \frac{\Delta f}{2 f_R}$, where Δf is the frequency bandwith between the two half power points and f_R the resonance frequency.

Therefore, by examining the magnitude of the imaginary part of the FRFs at a number of points on the structure, putting together the modal displacements at each point will create the mode shape.

2.4. Finite Element Model Updating

Model Updating study how modifications of the design variables will influence the system's response and how an error function that describes the deviation between analytical and experimental data, can be minimized. This process starts with a manual mass updating followed by sequentially validating and updating of modeling of mass, stiffness and damping using data from static and dynamic testing.

Reliability of a finite element model is only achieved with real information and with that data, the model will be validated and verified.

Complex non-linear structures, as in this study case, have some problems, such as manufacturing weight differences, faulty boundary conditions definition, incorrect assumptions of the material properties or difficulty in modelling shapes and joints. The long process of model updating ensures the quality of the matching between the real and numerical data [11].

A sensitivity analysis is performed to study what are the parameters that mostly affects the behaviour of the structure and then to present the discrepancy between the numerical and experimental values of the responses, different Correlation Criterions (CC) can be used for each update. CC will be interpreted as an objective function that needs to be minimized.

When the objective is updating the stiffness, the error function that must be minimized is the difference between experimental and analytical static displacements. For this case, the CC used was the CCDISP that measures the weigthed absolute relative difference between displacements.

After updating the stiffness based on static tests, the FRFs obtained from the GVT are important to update the mass and stiffness matrices.

The modal-based update can be performed using resonance frequencies only or adding modal displacements, MAC or POC. For this model updating, the CC used was the CCTOT that includes the CCABS for the resonance frequencies, CCMASS to converge the mass and CCMAC for the MAC.

3. Wing FEM

In order to perform pre testing static and vibration simulations, the usage of FEMs is common and the standard tool for structural analysis. It allows to have computational simulations that preliminary estimate the behaviour of a structure and help in detecting possible errors and optimizing conditions that can be truly precious for time and money savings.

Static loading structural simulations study the stiffness properties of a structure used to perform ultimate fracture analysis and displacement or torsion shape analysis. Dynamic analysis can output modal responses and help problems involving noise and fatigue damage.

This FEM was developed in *Ansys* software with shell elements for the surface skin and ribs and solid elements for the spars. Boundary conditions considered for both analysis were four holes on the spars that represent the assemblage points of the wing to the fuselage. Coordinate system uses X, Y and Z representing the longitudinal axis, yaw axis and spanwise direction, respectively.

Some preliminary differences, as expected in every experimental work, were detected even before testing the structure. The predicted mass of the wing should be 6.97 Kg and the result obtained with a scale was 11.15 Kg. Even after some calculations on the density, bonding resin, duratec, paint and non structural internals the deviation of the mass presents a 25% excess that was not accounted for in the model. The divergene of the mass was corrected before any computational analysis, changing the density of the composite from 1450 Kg/m^3 to 2162 Kg/m^3.

3.1. Static Analysis Results

The goal of the static analysis in this study is to simulate 30% or more of predicted deflection under the maximum operating load 2.5g's pull up manoeuvrer in flight. 4 different load cases were calculated on *Ansys*: 100N and 225N vertical load applied at the tip aligned with the aerodynamic center and 225N vertical load applied at the tip aligned with the aft spar and leading edge.

It was observed a maximum deflection at the tip of 3.7cm for the 100N loading case and 7.6cm for the 225N aligned with the aerodynamic center. Bending shapes and twist distributions can be visible in figure 1.

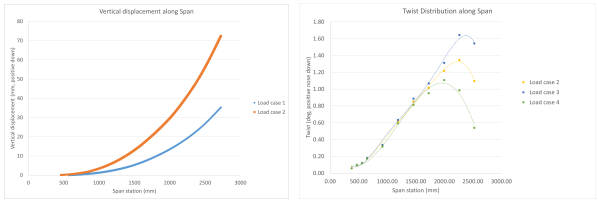

(a) Displacement along span (b) Twist variation along span

Figure 1: Static loading FEM analyses.

3.2. Modal Analysis Results

Modal analysis is important to choose where to install the sensors for the experimental tests in order to avoid nodal points. The results predict the first resonance frequency corresponding to the first bending mode around 9.6 Hz, the second frequency to the second bending mode around 37.8 Hz, the third frequency to the first in-plane mode around 42.1 Hz, the fourth frequency to the third bending mode around 92.2 Hz, the fifth frequency of 128.4 Hz to the second in-plane mode and finally the sixth mode corresponds to the first torsional mode around 153.3 Hz.

This results provide a first glimpse to check if the results obtained during GVT are similar. High differences in frequencies may indicate incorrect measurements that need to be repeated. Nevertheless, GVT results always have priority once validated.

4. Experimental Tests

4.1. Static Loading Tests

For each loading case, displacements of specific chosen points (fiducial stickers) along the wing surface will be measured in order to extract the bending and the twist deformation of the structure. It is important to know that in experimental wing loading tests, the presence of gravity can not be eliminated and for that reason should be considered.

The test plan starts with developing a jig that will be attached to an optical table and use four holes on the spars to fix the wing to the jig, upside down. Then, an aluminium part will be manufactured to fit in the tip of the wing with the purpose applying the load at three different chordwise positions: near the leading edge, the trailing edge and at the aerodynamic center. Load cases considered were the same as previously presented in section 3.1. Scanning of the original wing mounted on the jig without tip's loading and after unloading were done to have a reference point for the loading cases scans and the last one to check if any plastic deformation occured.

To measure the deflections 66 points were planned to be considered, 6 points chordwise in 11 sections along the span were considered, 3 points per section on the top surface and another 3 points per section on the bottom surface of the wing. 4 fiducial markers need to be sticked in a reference structure in order to provide a reference frame for the scanning. It was chosen to define the coordinate system on the jig to be always the same for all the different loading cases and not be affected by any displacements. The distribution of the stickers in the top surface and the coordinate system on the jig are visible in figure 2.

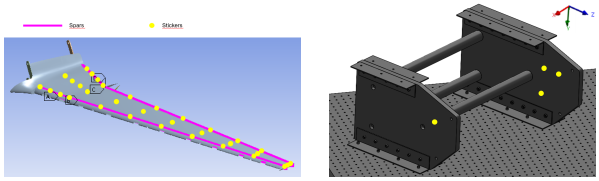

(a) Measurement stickers placement plan. (b) Coordinate system defined on the jig.

Figure 2: Fiducial stickers placement plan for the static tests.

Coordinate system used was the same as the presented in section 3.1 for the FEM analysis.

The heavy and unyielding jig was then manufactured and to provide adequate boundary conditions with tight tolerance, precise bushing were used to avoid displacements of the assembled surfaces. The assemblage of the wing mounted upside down on the jig and the fiducial markers placed along the wing as planned can be visible in figure 3. Along with the 3D scanning and to control unexpected excessive deflection, a ruler was placed behind the wing's tip to monitor the vertical displacement.

Load application was done by bolting a custom manufactured aluminium part to the winglet attachment box in the wing tip, visible on figure 3. A crate progressively filled with 2.5 Kg sand bags was hanged on this custom part in order to reproduce the FEM analyzed load cases. Between each load case, a 2,5 Kg increment loading strategy was implemented instead of direct loading the 10 or 22,5 Kg for systematic inspection in order to avoid possible failing of the structure. Both the costum part

and the cradle were accounted for the total load mass on the wing.

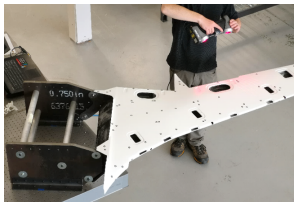

(a) Scanning of the mounted wing.

(b) Static tests setup with load applied on the tip.

Figure 3: Experimental Setup for Static Testing

After each load case, the fiducial stickers position on the wing is scanned. Comparing the position of these stickers from each load case to the first load case without load applied it is possible to find the displacements of the points.

The results represent the deflections between cases under load applied and the inital case without any loading at the tip. The post processing of the wing scans data showed a significant difference in vertical position between initial resting shape and post loading shape (about 16mm). However, it was confirmed that despite that difference, if rotated around the longitudinal axis of the reference coordinate system, the shapes of the initial and post loading structures were coincident. The structure experienced a rigid body rotation during the test. This suggests that probably a small displacement on the bonding between the attachment bushings and the spars occured, although not confirmed. Anyway, no permanent deformation was found.

In figure 4, it is visible that the wing is significantly stiffer than predicted. The expected vertical displacement at the wing tip is around 40% different when compared to the experimental results. Figure 5 shows that the pattern captured by the FEM is visible also in tests' resutls although with a different magnitude. It also shows that the torsional stiffness of the wing is under predicted by the FEM.

In conclusion, the experimental results show that the significant increase in structural mass is followed by a significant increase in torsional and bending stiffness of the wing.

4.2. Ground Vibration Tests

To study the dynamic behaviour of a structure, the extraction of modal parameters to validate the original model and perform any model update can be obtained from the post processing of the GVT results. During these tests resonance frequencies can be measured with high accuracy but limited in range. Less accurate results, but also possible to obtain, are mode displacements.

Noise sources that might happen are associated to: test configuration (fixtures, excitation tech-

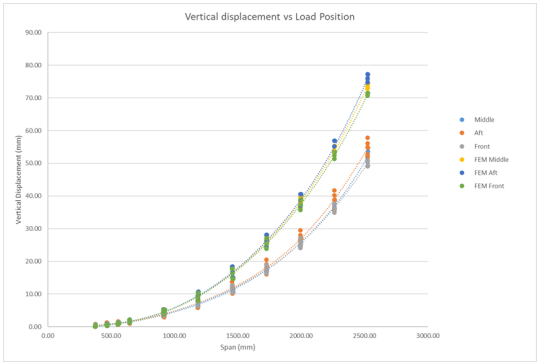

Figure 4: Comparison of experimental and FEM results for different loading cases.

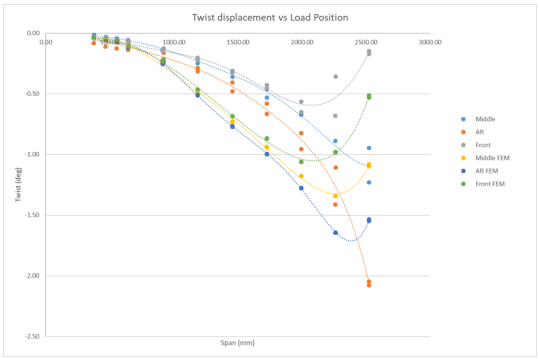

Figure 5: Comparison of experimental and FEM twist displacements for different load positions.

nique, locations of the measurements); calibration and distortions of the instrumentation and data acquisition system or eventual noise that can exist in the laboratory environment, that can be eliminated or improved with experience of the technician and extra care.

An important consideration during the test plan is to make sure the jig's natural frequencies will be far from the wing's frequency range of interest, 0Hz to 200 Hz.

In order to have redundancy on the results and different options to compare and choose the best outputs, 8 accelerometers should be used. Nevertheless, since the time consumption on model updating is high, only the best results' position are going to be used for that task. Sensor selection tools from *FEMtools* software were used to help finding the optimum placement of the tansducers. Accelerations were measured in two directions, X and Y. Z direction can be neglected because deflections are infinitesimal. An aluminium cube will need to be manufactured to guarantee the orthogonality of the sensors.

12 points were considered to choose which sensor location measures the less noisy results and 25 points will be impacted to improve the quality of the

mode displacements results. 12 equaly distributed points along the aft spar and 13 along the front spar lines, as visible in figure 6.

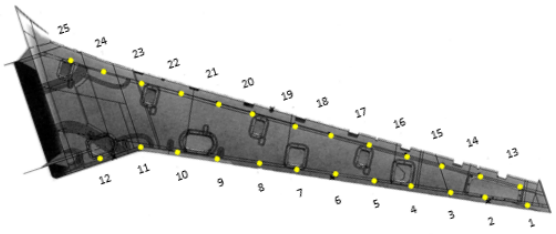

Figure 6: Roving impact DOFs for multi reference testing.

The experimental setup consists in the wing mounted in the same way as in the static loading tests. The instrumentation used to impact the structure was a PCB model 086C03 hammer with the medium impedance tip. PCB miniature single axis piezoelectric accelerometers model 352A24 were the available sensors used to measure the response of the structure to the impact. Data acquisition was accomplished using National Instruments (NI) 9234 IEPE acquisition cards connected to a NI cDAQ-9188 chassi. The PCB hammer and all the transducers are connected to the 9234 modules.

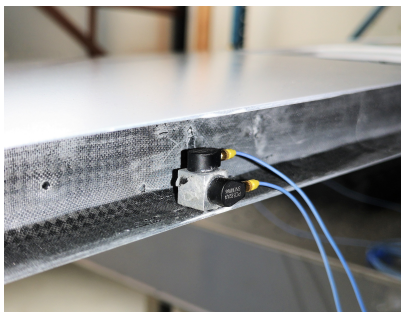

(a) PCB single axis piezoelectric accelerometers on the trailing edge.

(b) PCB hammer.

Figure 7: Intrumentation used on GVT.

The hammer technique consists in doing short, narrow pulse impacts, always perpendicular to the structure. FRF calculations are done by the *LabVIEW* software almost instantaneously when hitting the structure. To prevent errors or noise that may affect the results, 3 impacts needs to be done for the same DOF. It was decided to make a mesh refinement and instead of 25 impact points, 50 DOFs were impacted resulting in 100 FRF, 50 in Y direction and another 50 in X direction.

The raw data available on the testing interface is helpfull to monitor and improve the quality of the technique. All the FRFs acquired need be to curve fitted using *MEScope* software, by Vibrant Technology.

Note the relevance of measuring in the two directions. The peak around 50Hz, that corresponds to the first in plane mode, it is not visible in most of the FRFs obtained from the results of the accelerometer measuring Y direction. However, it is evident in all the results obtained with X direction measurements. An example of one FRF acquired is visible in figure 8.

Figure 8: Example of a post processed magnitude and phase graphs from a FRF result.

The clear way to analyse the peak frequencies is looking to the imaginary graph of the FRFs. An overlaid of all the imaginary part of 100 FRFs is visible in figure 9 and all the resonance frequencies can be evidently identified. In the bottom chart of the same figure, it is possible to see the output of the quick curve fitting function of *MEScope* software. The complex mode indicator function (CMIF) is calculated using the Polynomial method and all the peaks above the noise threshold line are counted.

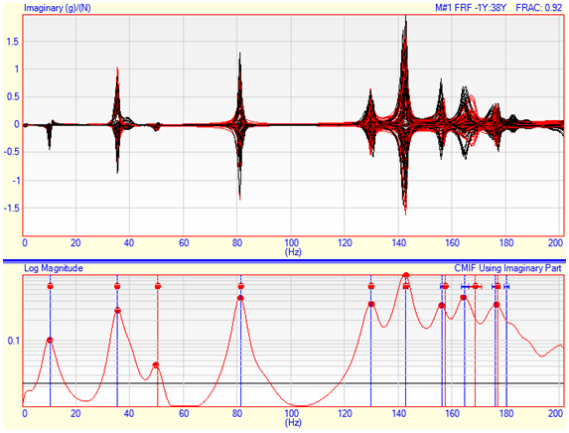

Figure 9: Automatic curve fitting function output of *MEScope* software used to determine the peaks correspondant to the natural frequencies.

This post processed data converged in the extraction of the modal parameters presented in table 1.

Table 1: FEM vs EMA resonance frequencies comparation.

Mode #	$FEA_f(Hz)$	$EMA_f(Hz)$	$EMA_{damping}(Hz)$	Δ_f
1	9.59	10.34	0.04	7.35
2	37.80	35.28	0.52	-6.60
3	42.09	50.38	0.66	19.75
4	92.17	81.34	0.43	-11.79
5	128.43	129.80	0.77	1.22
6	153.27	142.72	0.82	-6.70
7	153.27	157.48	0.67	2.43

It was expect to find differences in the same order of values when comparing GVT results with FEM results, however, the average difference between experimental and computational resonance frequencies is approximately 8.9%.

5. FEM update

The last step consists in performing a model updating study of a FEM. The model-based approach begins with the development of a computational model, such as a FEM based on design calculations, to be matched using structural parameters to the experimental tests data.

In this study, it was impossible to perform the analysis on the original FEM of the wing due to the large size of the original model. A new simplified FEM, visible in figure 10, needs to be developed in order to correlate data between computational and experimental tests. Sotware used to perform all the model updates was *FEMtools 4*, by Dinamic Design Solutions.

The final model should be accurate enough to be used in a future flutter analysis at critical speed.

Trying to keep the simplified beam model as close as possible to the original FEM of the wing, some characteristics were taken into account. Beam elements with rectangular cross section were used to connect the centroid of 50 wingbox's sections along the span. The reason to choose beam elements is that, even being simple and fast to compute in any FEM solver, they provide high fidelity results. The centroid's coordinates of the wingbox's sections were chosen to better represent the shape, sweep and dihedral angles of the wing over the span keeping also the same coordinate system.

The boundary conditions in this beam model are implemented by fixing the root node that will represents the 4 holes previously used in the more detailed FEM.

Values of Young's modulus and mass density were defined based in the properties of the constitution material of most of the wing. Young's modulus was defined as 67.1GPa and mass density as 2162 Kg/m^3.

In order to achieve a good pairing between responses, the beam model was discretized in 10 equally spaced sections along the span to give to the model more freedom to optimize the parameters in a distributed way over the span.

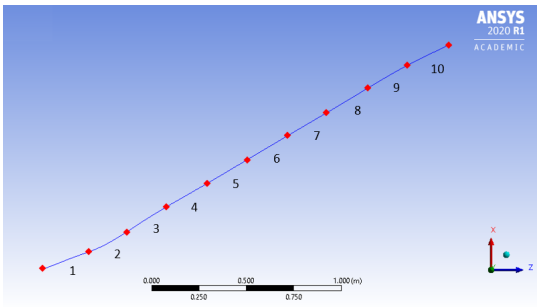

Figure 10: Beam FEM developed for the model update.

Young's modulus (E) and bending moments of inertia (Ix,Iy) were choosen for the update of the stiffness based on static loading tests results. The update of the dynamics of the structure based on GVT results considered the E, Ix, Iy, cross section area (A) and mass density (ρ). Many iterations were performed varying the number of parameters used for the update to understand which of them are fundamental to converge the responses and which can output more interesting results.

Preliminary updates of the cross section area and moments of inertia were manually done. These values are not a perfect representation of the structure but they can be an initial a good aproximation of the distribution of these parameters along the span.

5.1. Based on Static Tests Results

The data from the static loading tests that will be used is referred to the third scanning case results correspondent to the 22.5 Kg load applied at the wing tip's aerodynamic center. CCDISP CC converged after 10 iterations in 3,1%, as visible in figure 11, which means an average similarity between responses of 96.9 %.

It is important to highlight the differences between initial and updated parameters of Young's modulus in specific sections of the wing that is two orders of magnitude lower. A possible explanation for this fact is that the sensitivy to this parameter is higher than for the moments of inertia.

5.2. Based on GVT Results

After updating the beam FEM with the results obtained from the static tests, one can assume a reliable stiffness pairing between computational and real model. Different starting points will be studied for the dynamic update to understand which parameters are more sensitive and outputs the best results.

Three updates using the initial FEM and four

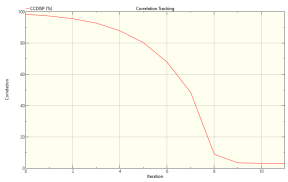

(a) CC CCDISP convergence.

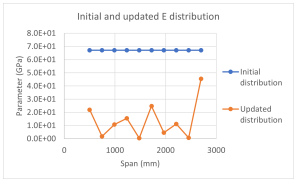

(b) Young's modulus.

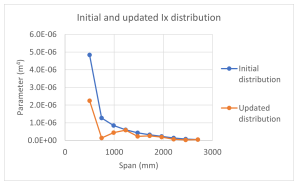

(c) Moment of inertia x.

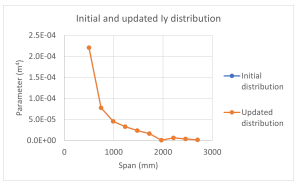

(d) Moment of inertia y.

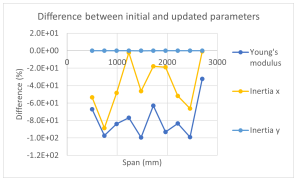

(e) Differences between initial and updated FEM.

Figure 11: CC and initial and updated parameters distribution for the first model update based on static load test results.

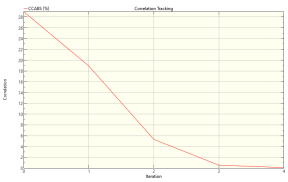

(a) CC CCABS convergence.

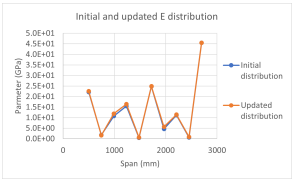

(b) Young's modulus.

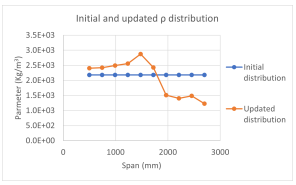

(c) Mass density.

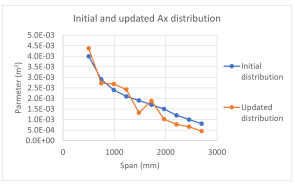

(d) Cross section area.

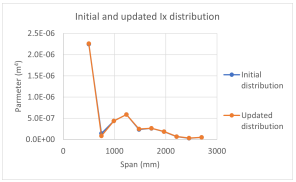

(e) Moment of inertia x.

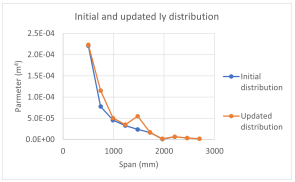

(f) Moment of inertia y.

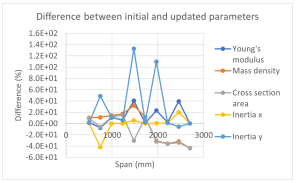

(g) Differences between initial and updated parameters distribution.

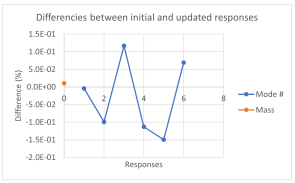

(h) Differences between initial and updated response distribution.

Figure 12: CC, initial and updated parameters distribution and response values for the model update based on GVT data starting with the updated FEM.

using the updated FEM were studied varying the chosen parameters. Initial FEM presents approximately 341% of average difference and updated FEM of 27% when compared to the test frequencies.

Responses considered were the mass of the model and the first sixth frequencies from the first bending till the first torsion mode.

The case that achieved the best result had the E, ρ, A, Ix, Iy free to update starting with the stiffness updated FEM. The CC CCABS achieved matching results and the responses' differences between FEM and experimental results converged in an average value of 99.9% of similarity. The E has not changed significantly, which means that the stiffness update results can be confirmed when pairing with GVT data. The higher percentual differences are now present on the bending moment of inertia about Y axis, although not deemed as very significant given the lack of sensitivity to this parameter observed previously.

6. Conclusions

The goals were successfully achieved starting with the FEM analyses followed by the experimental work, static tests and GVT to characterize the stiffness and correlate the modal dynamics of the wing, respectively.

Since GVT is more time consuming and expensive than a static load test, one of the main goals of ground structural testing was to prove, when comparing the results of both tests, if it is reliable to validate the FEM model only resorting to static loading tests. From this experimental work results, it should be highlighted that the results of the static loading test are not proportional to the GVT's results. The expected vertical displacement at the wing tip is around 40% different when compared to the experimental results and for that reason, a significant increase in torsional and bending stiffness of the wing due to the significant increase in structural mass was observed. The average difference between experimental and computational resonance frequencies is approximately 8.9%.

This difference values totally disprove the previous hipothesis. Having an increase in the stifness of the wing haven't affected that much the modal response. With this, it is imperative to perform both tests without the possibility of using one to replace

the other.

A beam model was generated and a study on the model updating process of a FEM was performed varying the chosen parameters. Different obtained FEMs accuratly represent the behaviour of the structure. However, some difficulties were found when trying to match the mode shapes of the structure.

A continuation of this work can go through generating a more complex and elaborated FEM, without compromising the capabilities of the software, but that is capable of improving the matching of the mode shapes. A suggestion for this process can be to change the type of elements used to create the simplified FEM.

Once this perfect matching is achieved, aeroelastic flutter calculations can be performed to study the dynamic instabilities of the wing.

Acknowledgements

The author would like to thank Prof. Afzal Suleman for this opportunity and all the UVic-Cfar team, specially Stephen Warwick for the technical support and Dr. José Vale for the co-mentoring.

References

[1] Zhenli CHEN, Minghui ZHANG, Yingchun CHEN, Weimin SANG, Zhaoguang TAN, Dong LI, and Binqian ZHANG. Assessment on critical technologies for conceptual design of blended-wing-body civil aircraft. *Chinese Journal of Aeronautics*, 32(8):1797–1827, 2019.

[2] S. L. Yang, M. A. Page, and E. J. Smetak. Achievement of NASA new aviation horizons N+2 goals with a blended-wing-body X-plane designed for the regional jet and single-aisle jet markets. In *AIAA Aerospace Sciences Meeting, 2018*, number 210059, 2018.

[3] Masoud Sanayei, Ali Khaloo, Mustafa Gul, and F Necati Catbas. Automated finite element model updating of a scale bridge model using measured static and modal test data. *Engineering Structures*, 102:66–79, 2015.

[4] Nathan Richards Fields. Advantages and challenges of unmanned aerial vehicle autonomy in the postheroic age. Master's thesis, James Madison University, 2012.

[5] Jonathan E. Cooper Jan R Wright. *Introduction to Aircraft Aeroelasticity and Loads*. John Wiley Sons, Ltd., 2007.

[6] Michael A. Sutton, Jean-José Orteu, and Hubert W. Schreier. *Image Correlation for Shape, Motion and Deformation Measurements*. Springer, 2009.

[7] Hubert Schreier, Jean-José Orteu, and Michael A. Sutton. *Image Correlation for Shape, Motion and Deformation Measurements*. Springer, Boston, MA, 2009.

[8] Jamey D. Jacob, Suzanne W. Smith, Dave Cadogan, and Steve Scarborough. Expanding the small UAV design space with inflatable wings. *SAE Technical Papers*, (724), 2007.

[9] Stephen Daniel Wilfred Warwick. Measurement of Aeroelastic Wing Deflections on a Remotely Piloted Aircraft using Modal Strain Shapes. Master's thesis, University of Victoria, Canada, 2020.

[10] M. Peeters, G. Kerschen, and J. C. Golinval. Dynamic testing of nonlinear vibrating structures using nonlinear normal modes. *Journal of Sound and Vibration*, 330(3):486–509, 2011.

[11] José Carlos Carregado. Static and Dynamic Characterization of a Flexible Scaled Joined-Wing Flight Test Demonstrator. Master's thesis, Instituto Superior Técnico, Lisbon, 2017.

[12] Anders Brandt. *Noise and Vibration Analysis: Signal Analysis and Experimental Procedures*. John Wiley Sons, Ltd., 2011.

[13] Irving Ojalvo and Miya Newman. Vibration modes of large structures by an automatic matrix-reduction method. *American Institute of Aeronautics and Astronautics*, 8:1234–1239, 07 1970.

[14] J. Cooley and John W. Tukey. An algorithm for the machine calculation of complex fourier series. *Mathematics of Computation*, 19:297–301, 1965.

[15] SIEMENS SIMCENTER. What is a frequency response function (frf)? https://community.sw.siemens.com/s/article/what-is-a-frequency-response-function-frf, 2020. (accessed: 07.11.2020).

[16] Nuno Mocho Simões. Design of a Ground Vibration Test Certification System For Unmanned Air Vehicles. Master's thesis, Instituto Superior Técnico, Lisbon, 2015.